Summer Program Participation Report

GSI HELMHOLTZ CENTRE FOR HEAVY ION RESEARCH





Prepared by
Thanaporn Chimruang


According to Her Royal Highness Princess Maha Chakri Sirindhorn's Royal Initiatives in 2025

Introduction

This report serves as a summary document detailing the results and experiences gained from participating in the GSI Helmholtz Centre for Heavy Ion Research Summer Student Program in Darmstadt, Germany. The program ran for eight weeks, from July 20th to September 13th, 2025. This document compiles the author's academic perspectives, research contributions, and personal reflections throughout the residency. The research component focuses on a theoretical project conducted within the GSI framework. The author and committee hope that this report will be informative and inspiring for future applicants, highlighting the valuable opportunity to gain international research experience and broaden horizons abroad.

Thanaporn Chimruang
Walailak University

Contents

Table of Contents i

List of Figures iii

Acknowledgement iv

1 GSI-FAIR 1
- 1.1 The GSI Helmholtz Centre for Heavy Ion Research . . . 1
- 1.2 The GSI Summer Student Program . . . 3

2 Program Schedule and activities 4
- 2.1 Educational Structure and Research Work . . . 6
- 2.2 Research Placement and Supervision . . . 6
- 2.3 Program Conclusion . . . 6
- 2.4 Academic Program and Facility Tours . . . 7
  - 2.4.1 Accelerators: From the Source to the Target . . . 7
  - 2.4.2 Materials Research . . . 7
  - 2.4.3 ROOT Software Tutorial . . . 7
  - 2.4.4 Experimental Hadron Spectroscopy . . . 8
  - 2.4.5 Biophysics & Cancer Therapy with Heavy Ions . . . 9
  - 2.4.6 Visit of Green Cube and FAIR Viewing Platform . . . 9
  - 2.4.7 Hadron Physics with Anti Protons II . . . 9
  - 2.4.8 Plasma Physics with Intense Ion Beams . . . 10
  - 2.4.9 Plasma Physics with Intense Laser Beams . . . 10
  - 2.4.10 Visit of CryRing and HADES . . . 10
  - 2.4.11 Atomic Physics . . . 11
  - 2.4.12 Visit of Ion Sources and UNILAC . . . 11
  - 2.4.13 Visit of FAIR Construction Site . . . 12
- 2.5 Activities . . . 12
  - 2.5.1 Pedestrian rally in Darmstadt . . . 12
  - 2.5.2 BBQ Grill and Chill Party . . . 13
  - 2.5.3 Ioni Summer Cup: Sports Fun Event . . . 14
  - 2.5.4 Annual Workshop & Grill and Chill . . . 15

3 Research Overview 16
- 3.1 Background and Motivation . . . 16
- 3.2 Objectives . . . 17
- 3.3 Related Theories . . . 17
  - 3.3.1 Charm Quarks in High-Energy Collisions . . . 17
  - 3.3.2 The Statistical Hadronization Model (SHM) . . . 18
    - 3.3.2.1 Canonical Ensemble and Hadron Multiplicity . . . 18
- 3.4 Results and discussion . . . 19
  - 3.4.1 Determining Input Parameters for the SHM . . . 19
  - 3.4.2 Model-Based Input Multiplicities . . . 19
  - 3.4.3 Thermal Parameter Extraction . . . 20

3.4.4 Predicted Particle Multiplicities . . . 21
3.4.4.1 Normal Hadron Multiplicities . . . 22
3.4.4.2 Charm Multiplicities . . . 22
3.4.4.3 Exotic Multiplicities . . . 24
3.4.4.4 Nuclei Multiplicities . . . 25
3.4.5 Particle Multiplicity vs. Baryon Number . . . 26
3.4.6 Comparison with Other Systems . . . 27
3.4.6.1 Proton-Gold (p+Au) Collisions . . . 27
3.4.6.2 Pb+Pb Collisions at LHC Energy . . . 27
3.4.7 Conclusion . . . 28

4 Experiences **29**
4.1 Cycling Culture . . . 29
4.2 Excursion to Frankfurt . . . 29
4.3 Excursion to Bonn and Hiking the Löwenburg . . . 30
4.4 Hiking to Frankenstein Castle . . . 30
4.5 Relaxing by the River . . . 31
4.6 Farewell Meals and Culinary Exchange . . . 32
4.7 Photo with My tutor . . . 33

5 Appendix **34**

List of Figures

1.1 Schematic layout of the GSI and FAIR accelerator facilities. 2

2.1 Accelerators Lecture 8
2.2 Materials Research Lecture 8
2.3 ROOT Tutorial guideline 8
2.4 ROOT Program 8
2.5 The Green Cube data center at GSI 10
2.6 The ongoing FAIR construction site 10
2.7 The CRYRING facility 11
2.8 The HADES Experiment 11
2.9 The real structure of Hydrogen (Atomic Physics Lecture) 11
2.10 The Universal Linear Accelerator (UNILAC) 12
2.11 The Ion Sources 12
2.12 The personal protective equipment 13
2.13 The SIS100 accelerator 13
2.14 Pedestrian rally in Darmstadt 13
2.15 BBQ Grill and Chill Party 14
2.16 Ioni Summer Cup: Sports Fun Event 14
2.17 Grill and Chill party 15
2.18 The Silicon Target 15

3.1 Chemical freeze out Temperatures and Baryon Chemical Potentials for Au+Au collisions at different centralities. 20
3.2 Predicted(lines) and Input(markers) normal hadron multiplicities in Au+Au collisions. 22
3.3 Predicted(lines) and Input(markers) charm multiplicities in Au+Au collisions. 23
3.4 Predicted(lines) and Input(markers) exotic multiplicities in Au+Au collisions. 24
3.5 Predicted(lines) and Input(markers) nuclei multiplicities in Au+Au collisions. 25
3.6 Particle multiplicities as a function of Baryon Number for Au+Au and Pb+Pb collisions. 26

4.1 Daily life during the program with bicycle 29
4.2 The Euro currency landmark in Frankfurt 30
4.3 Hiking the Löwenburg 31
4.4 Hiking to Frankenstein Castle 31
4.5 The Main River in Frankfurt. 32
4.6 My roommate 33
4.7 The plenty of food 33
4.8 My tutor is in the middle 33

Acknowledgement

The author wishes to express profound gratitude for the support that made the successful completion of this Summer Student Program possible.Foremost, this experience would not have been possible without the great benevolence of Her Royal Highness Princess Maha Chakri Sirindhorn, who graciously provides opportunities for Thai students to study, learn, and expand their knowledge in scientific research collaboration with world-class scientists and institutions. The experience gained from participation in this program is invaluable, serving as a catalyst for personal growth, career advancement, and contributing to the social development of the nation.

Additionally, I extend my sincere thanks to the selection committee, all responsible officers, and the supporting organizations, including the Princess Maha Chakri Sirindhorn Foundation for Heavy Ion Research (PMCSHIF), the National Science and Technology Development Agency (NSTDA), and the Synchrotron Light Research Institute (SLRI), for their invaluable moral and financial support. This effort promotes and fosters high-level cooperation between Thailand and the GSI research institute for the sustained benefit of Thai science.Finally, heartfelt gratitude is extended to the Federal Government of Germany and the State of Hesse for their essential support in covering daily living expenses throughout the duration of the program.

Thanaporn Chimruang
Walailak University

Chapter 1

GSI-FAIR

1.1 The GSI Helmholtz Centre for Heavy Ion Research

The GSI Helmholtz Centre for Heavy Ion Research (GSI) is one of the world's leading laboratories in heavy-ion physics, located in Darmstadt, Germany. The institute is internationally recognized for its unique capability to produce a wide variety of ion beams — ranging from light ions such as hydrogen to very heavy ions like uranium. This broad ion spectrum enables GSI to conduct cutting-edge experiments in both fundamental and applied physics.

The main research tools at GSI are its large-scale particle accelerators, which include the Linear Accelerator and the Heavy-Ion Synchrotron SIS18. Within these facilities, heavy ions are accelerated to velocities approaching the speed of light and directed onto fixed targets. These interactions allow scientists to study the fundamental properties of matter in fields such as nuclear physics, nuclear astrophysics, and atomic physics. In addition, GSI carries out research with applications in material science, plasma physics, biophysics, accelerator technology, and radiation protection.

Currently, GSI is being expanded through the construction of the FAIR (Facility for Antiproton and Ion Research) project — one of the largest research infrastructures for nuclear and particle physics worldwide. FAIR will include a new set of synchrotrons, SIS100 and SIS300, with a total circumference of about 1,100 m, capable of accelerating ions to even higher energies than before. As of 2025, the FAIR complex is in its final stages of construction and is expected to open in the near future. Once operational, FAIR will enable unprecedented investigations into the properties of matter under extreme conditions.

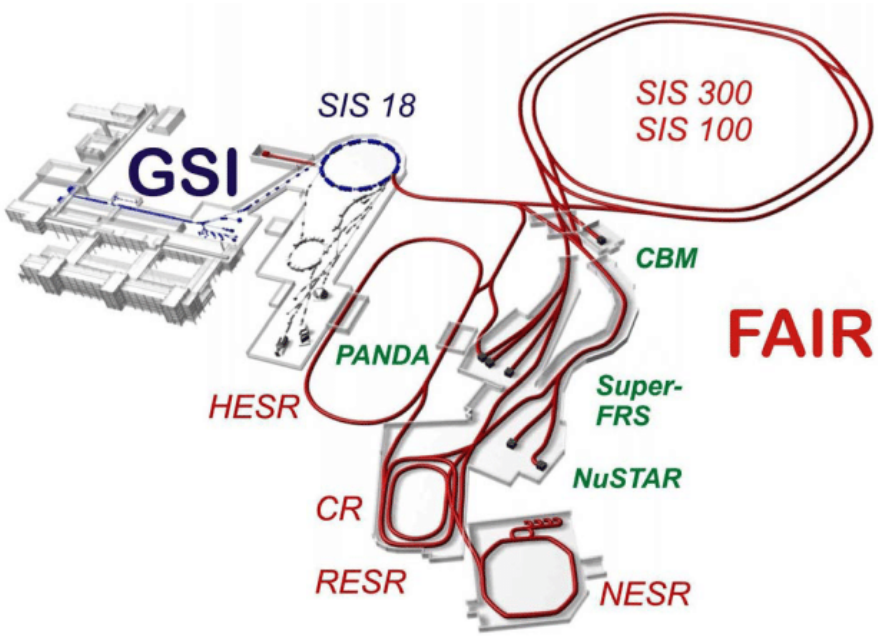

Figure 1.1: Schematic layout of the GSI and FAIR accelerator facilities.

Figure 1.1 illustrates the layout of the GSI–FAIR accelerator complex. The existing SIS18 synchrotron at GSI (blue) serves as the injector for the new FAIR accelerators SIS100 and SIS300 (red). The high-energy beams will then be delivered to various experimental stations, including:

- PANDA (AntiProton ANnihilation at DArmstadt) for studying antiproton–proton interactions and hadron structure.
- CBM (Compressed Baryonic Matter) for investigating matter at high baryon densities.
- Super-FRS (Superconducting Fragment Separator) for isotope separation and rare-nucleus research
- NuSTAR (Nuclear Structure, Astrophysics and Reactions) for exploring nuclear properties relevant to astrophysical processes.

Additional beamlines and storage rings such as CR, HESR, RESR, and NESR will provide beam cooling, collection, and manipulation to meet the requirements of each experiment. Together, these facilities demonstrate the close integration between the existing GSI infrastructure and the forthcoming FAIR complex.

1.2 The GSI Summer Student Program

The GSI Summer Student Program is an annual international research program designed for undergraduate (3rd–4th year) and master's students from European countries and partner institutions worldwide. The program offers participants the opportunity to work on real research projects within the GSI–FAIR research groups under the supervision of experienced scientists and tutors.

During the eight-week program, students engage in hands-on research, attend scientific lectures from GSI and FAIR experts, and participate in laboratory tours that provide insights into advanced experimental facilities. The program also features social and cultural activities such as the city rally in Darmstadt, BBQ parties, and sports competitions to foster interaction and collaboration among participants from diverse cultural and academic backgrounds.

In 2025, the program took place from July 20 to September 13, with students from many countries participating. Accommodation was provided at the Arheilger Hof Hotel, located about 4 km from the GSI campus, where students lived and shared their experiences throughout the summer.

During the seventh week, each student was required to submit a written research report summarizing their project results, followed by a final presentation in the eighth week, which marked the culmination of the program. These presentations provided a valuable platform for exchanging ideas and discussing results with scientists from multiple disciplines.

This report summarizes the author's experience in the 2025 GSI–FAIR Summer Student Program. Chapter 2 provides an overview of the weekly activities and events throughout the program. Chapter 3 presents an overview of the research project carried out during the stay. Chapter 4 reflects on life experiences and personal development during the program. The Appendix includes the full version of the research report submitted to GSI.

Chapter 2

Program Schedule and activities

Table 2.1: Summer Program Complete Schedule (Weeks 1 - 8)

1st week		
Mon, 21.07.25	9:30-11:00	Registration: Main lecture hall
	11:00-12:30	Welcome address and first meeting of students
	14:30-16:00	Accelerators: from the source to the target
	16:15	Welcome reception with tutors
Tue, 22.07.25	9:15-10:15	Materials Research
	10:30-12:00	Compressed Nuclear Matter I (Introduction to relativistic nucleus-nucleus collisions)
	13:30	Group Photo
Wed, 23.07.25	9:30	First Project Day
	9:30-12:30	ROOT tutorial (non public)
Thu, 24.07.25	9:30-12:30	ROOT tutorial (non public)
Fri, 25.07.25	9:15-10:15	Experimental Hadron Spectroscopy
	10:30-11:30	Biophysics & Cancer Therapy with Heavy Ions
	11:30-12:15	Visit of Green Cube
	13:30-14:30	Visit of Medical Cave and FAIR Viewing Platform
Sat, 26.07.25	9:30-15:30	Pedestrian rally in Darmstadt
2nd week		
Tue, 29.07.25	9:15-10:15	Hadron Physics with Anti_Protons II (Instrumentation)
	10:30-11:15	Plasma Physics with Intense Ion Beams
	11:30-12:15	Plasma Physics with Intense Laser Beams
	16:00-17:30	Visit of CryRing and HADES
Fri, 1.08.25	9:15-10:15	Atomic Physics
	10:30-11:00	International Recruiting Programs at FAIR/GSI

	13:30-15:30	Visit of Ion sources, UNILAC, Main Control & SHIP/SHIPTRAP
3rd week		
Tue, 5.08.25	9:15-12:30	Tutorial: Scientific Writing/ Latex Course
Fri, 8.08.25	14:00-15:00	Nuclear Structure and Astrophysics I
4th week		
Tue, 12.08.25	10:30-11:30	Nuclear Structure and Astrophysics III (Experiments at the ESR)
	11:30-13:00	Visit of FRS and ESR
Fri, 15.08.25	9:15-12:30	Tutorial: Scientific Presentations
	14:00-15:00	Nuclear Structure and Astrophysics II
5th week		
Tue, 19.08.25	11:00-12:00	Superheavy Element Research
Fri, 22.08.25	8:00-10:00	Visit of FAIR (Group I)
	10:00-12:00	Visit of FAIR (Group II)
	15:15	Ioni Summer Cup: Our Sports Club invites all Summer Students and Tutors to an Event
6th week		
Tue, 26.08.25	9:15-10:15	Computing for experiments
	10:30-12:00	Impact to the Society
Fri, 29.08.25	9:15-10:15	Compressed Nuclear Matter II (Dilepton & Strangeness Production)
	10:30-11:30	Compressed Nuclear Matter III (Results from ALICE at LHC)
7th week		
8th week		
Mon, 8.09.25	10:00-17:00	Reports of the Students on their projects
Tue, 9.09.25	10:00-17:00	Reports of the Students on their projects
Wed, 10.09.25	10:00-17:00	Reports of the students on their projects
Thu, 11.09.25	9:00-10:00	Final Meeting (obligatory)
	17:00-22:45	Farewell dinner
Fri, 12.09.25		END of the PROGRAM/ Departure day

2.1 Educational Structure and Research Work

The program's educational component was highly concentrated during the initial weeks.

- Weeks 1 and 2 (Intensive Lectures): The first two weeks were dedicated to daily lectures held in the Lecture Hall. These sessions covered a broad range of topics related to GSI-FAIR research, with several lectures directly relevant to the theoretical project the author was assigned. Consequently, attendance at these daily lectures was mandatory and highly beneficial.
- Weeks 3 to 8 (Focused Research): The lecture schedule was reduced to two mandatory sessions per week (on Tuesdays and Fridays) from the third week onwards. This shift allowed for a primary focus on research execution.

2.2 Research Placement and Supervision

The author was integrated into the Theoretical Physics Group, located on the second floor of the same building as the Lecture Hall. The research project was specifically focused on Particle Physics, aligning with the core theoretical investigations at GSI.

The reduced lecture schedule facilitated close supervision. The author's supervisor (tutor) typically scheduled advisory meetings at GSI exclusively on days when the author did not have mandatory lectures, ensuring dedicated time for guidance and discussion of results. Furthermore, the supervisor occasionally arranged travel to Goethe University in Frankfurt for collaborative discussions, where the research results were shared and reviewed with other academic personnel.

2.3 Program Conclusion

The final two weeks of the program were reserved for synthesis and presentation:

- Week 7 (Report Submission): This week was kept free of scheduled activities, allowing all students dedicated time to finalize and submit their comprehensive research reports.
- Week 8 (Final Presentations): The program culminated in a formal symposium where all students presented the results of their eight-week research projects to the GSI-FAIR scientific community.

2.4 Academic Program and Facility Tours

2.4.1 Accelerators: From the Source to the Target

This lecture provided a comprehensive overview of the entire particle acceleration chain within the GSI and FAIR infrastructure. The session traced the ion path from its initial creation to its final collision with the target, covering the fundamental process of converting raw materials into high-energy ion beams.

Ion Sources and UNILAC: The process begins at the ion sources, followed by the Universal Linear Accelerator (UNILAC), which provides the crucial initial acceleration phase. The UNILAC brings the heavy ions to a sufficient energy level for efficient injection into the subsequent ring systems.

Synchrotron Systems: The lecture focused on the operation of the existing SIS18 and the upcoming SIS100 (a core component of the FAIR project). These Synchrotrons utilize powerful magnetic fields and RF cavities to guide and boost the energy of heavy ions up to relativistic speeds before delivering them precisely to the experimental targets.

2.4.2 Materials Research

The Materials Research session explored the vast applications of GSI's unique high-energy heavy ion beams within materials science and technology. The core focus was on Ion-Matter Interaction Processes (illustrated in Figure 2.2, which details the fundamental physics of how heavy ions transfer energy to a material matrix. The two primary mechanisms discussed were Electronic Stopping, where energy transfer mainly causes ionization and electronic excitation, and Nuclear Stopping, which results in direct atomic displacement and collision cascades.

Crucially, the lecture emphasized that the final modification state of the material, which is key to applications like nanostructure engineering and assessing radiation hardness, is determined by the precise balance between these two energy transfer processes.

2.4.3 ROOT Software Tutorial

This two-day session provided a practical introduction to the ROOT data analysis framework, which is widely used in high-energy and nuclear physics.

Day 1: Setup and Basics: The first day was focused on the technical foundations, including learning about the software's architecture, essential commands, and the successful installation and configuration of the program environment.

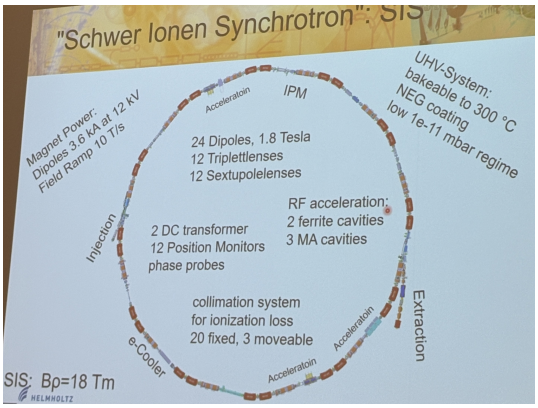

Figure 2.1: Accelerators Lecture

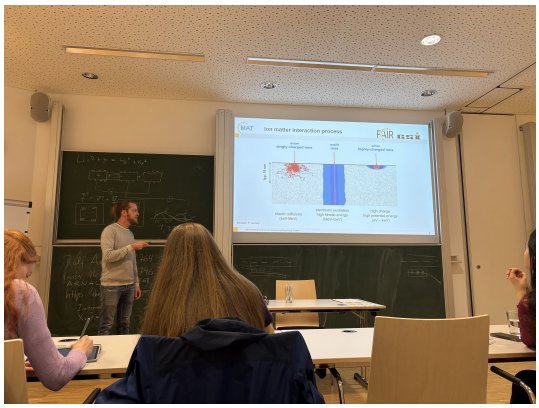

Figure 2.2: Materials Research Lecture

Day 2: Practical Application: The second day transitioned into hands-on experimentation. Participants worked through simple commands and basic programming logic within the ROOT environment, concluding with practical exercises such as plotting fundamental mathematical functions to familiarize themselves with the graphical output capabilities of the software.

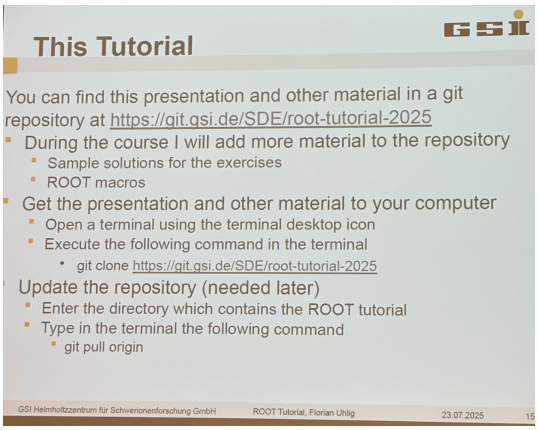

Figure 2.3: ROOT Tutorial guideline

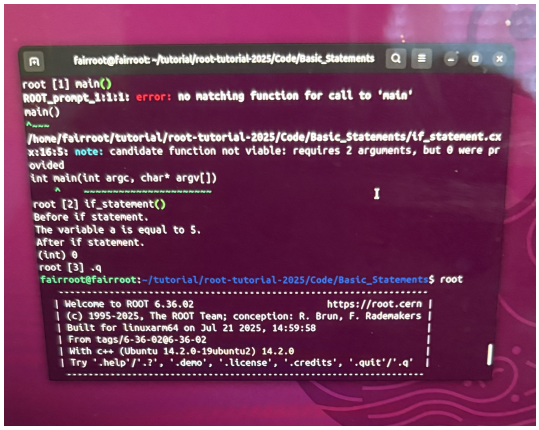

Figure 2.4: ROOT Program

2.4.4 Experimental Hadron Spectroscopy

This lecture provided a detailed overview of the experimental field of hadron spectroscopy, specifically focusing on the ongoing search for and study of exotic states. The session outlined the techniques used to precisely measure the properties (mass, spin, and parity) of known hadrons, which follow the traditional three-quark (qqq) or quark-antiquark ($q\bar{q}$) configurations.

Crucially, the discussion then pivoted to identifying predicted states that do not fit the conventional quark model, such as tetraquarks ($qq\bar{q}\bar{q}$), pentaquarks ($qqqq\bar{q}$), and glueballs (states composed entirely of gluons). The lecture connected these theoretical predictions to key experimental facilities, emphasizing the role of

the PANDA experiment at FAIR and its use of antiproton beams to explore the charm sector, which is essential for discovering these rare, novel configurations of quarks and gluons.

2.4.5 Biophysics & Cancer Therapy with Heavy Ions

One of GSI's most significant applied research fields is Biophysics, focusing primarily on the development of cancer therapy using heavy ions (such as carbon ions). This method capitalizes on the Bragg peak phenomenon, which allows the energy dose to be precisely concentrated within the tumor while sparing surrounding healthy tissue, a key advantage over conventional X-ray radiation. GSI pioneered this technique globally, with trials leading to the establishment of the Heidelberg Ion-Beam Therapy Center (HIT) for routine patient treatment.

Beyond clinical success, the biophysics program investigates the fundamental biological effects of ion radiation on DNA and repair mechanisms. The future FAIR accelerator will enhance this research by delivering higher-intensity beams for advanced radiobiological studies. This work underscores the direct contribution of fundamental heavy-ion physics to medical innovation.

2.4.6 Visit of Green Cube and FAIR Viewing Platform

2.5 The interior of the Green Cube data center at GSI, showcasing rows of server racks and cooling infrastructure. The Green Cube houses the critical computing resources and high-performance computing clusters necessary for processing data from current and future FAIR experiments.

2.6 An external view of the ongoing FAIR construction site, illustrating the scale of the future facility under a major cloud formation. The foreground highlights a schematic overview of the GSI and FAIR accelerator facilities, including the SIS100 ring and the locations of key experiments such as CBM and PANDA.

2.4.7 Hadron Physics with Anti Protons II

This lecture, the second part focusing on Hadron Physics with Antiprotons, provided a technical overview of the sophisticated instrumentation required for experiments utilizing antiproton beams. The session specifically highlighted the PANDA (Anti-Proton Annihilation at Darmstadt) experiment, a core component of the FAIR facility. The discussion covered the design and functionality of the PANDA detector system, which is optimized to achieve high luminosity and energy resolution necessary for the precise spectroscopy of charmed and exotic hadrons.

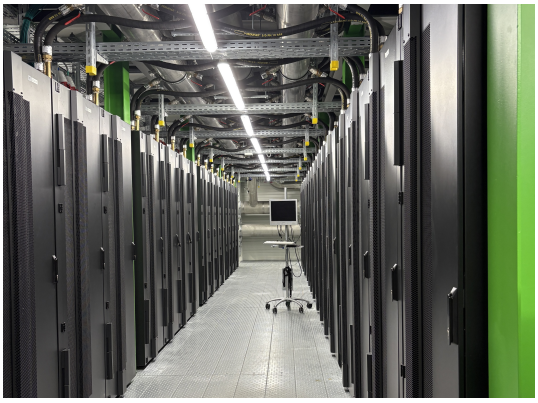

Figure 2.5: The Green Cube data center at GSI

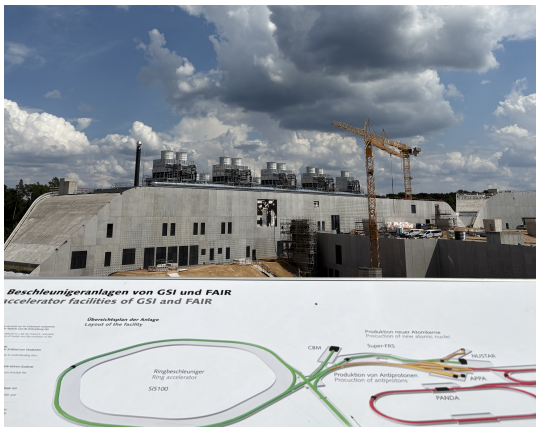

Figure 2.6: The ongoing FAIR construction site

2.4.8 Plasma Physics with Intense Ion Beams

This lecture focused on the interaction between intense ion beams and plasma, emphasizing the fundamental physics governing beam-plasma coupling, instabilities, and energy deposition. Applications in inertial confinement fusion (ICF) and materials research were discussed, highlighting how ion beams can be used to create and diagnose high-energy-density plasma states. The session provided insights into experimental techniques and simulation tools used to model plasma behavior under extreme conditions.

2.4.9 Plasma Physics with Intense Laser Beams

The session explored how high-power laser beams interact with matter to produce plasma, with particular attention to nonlinear effects, laser absorption, and plasma instabilities. The applications of laser-driven plasmas in fusion research, particle acceleration, and astrophysical modeling were introduced. The lecture also emphasized the importance of precise laser control and diagnostic systems in studying ultrafast plasma dynamics.

2.4.10 Visit of CryRing and HADES

The visit included the CRYRING facility (2.7), which is an existing synchrotron-storage ring complex now integrated into the FAIR development. The CRYRING is designed for high-precision experiments involving highly charged ions and molecular ions at low energies.

The second part of the visit focused on the High Acceptance Di-Electron Spectrometer (HADES) experiment (2.8), located at the SIS18 accelerator. HADES is a key fixed-target experiment dedicated to studying the properties of hadrons in

nuclear matter and the production of electron-positron pairs (e^+e^-) from elementary and heavy-ion collisions.

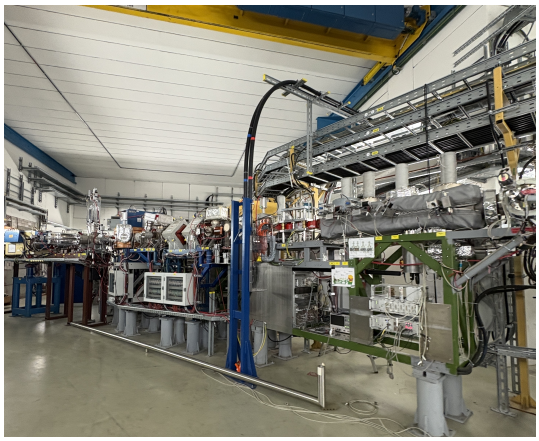

Figure 2.7: The CRYRING facility

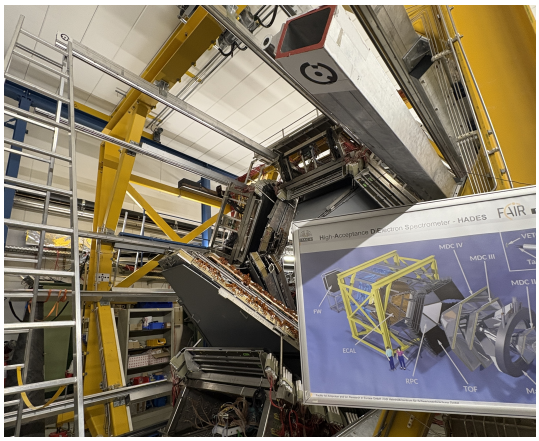

Figure 2.8: The HADES Experiment

2.4.11 Atomic Physics

This lecture provided an in-depth exploration of the real structure of the hydrogen atom, moving beyond the simple Bohr model to discuss modern quantum mechanics. The session detailed the progressive splitting of energy levels, starting with the *Schrdinger* equation (Bohr energy levels), and sequentially introducing increasingly refined effects.

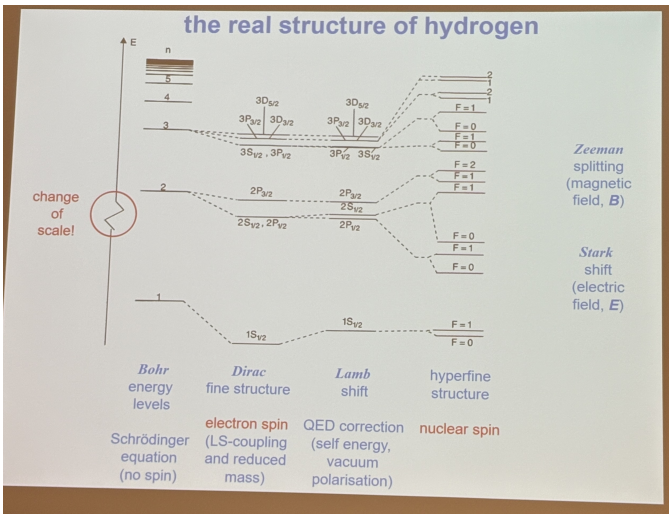

Figure 2.9: The real structure of Hydrogen (Atomic Physics Lecture)

2.4.12 Visit of Ion Sources and UNILAC

The visit began to the Universal Linear Accelerator (UNILAC) (2.10), which serves as the powerful first-stage accelerator. The UNILAC accelerates the ions to

a high enough energy level for efficient injection into the subsequent synchrotron ring systems (SIS18 and SIS100). The tour provided a view of the long, segmented structure of the LINAC system and its necessary RF and vacuum infrastructure.

The tour continued at the Ion Sources (2.11), where the raw material is converted into a plasma state to generate the specific ion species required for experiments. These sources are capable of producing a wide variety of positive ions, from light elements up to uranium. This complex process is critical for achieving the high beam intensities needed for modern nuclear physics research.

Figure 2.10: The Universal Linear Accelerator (UNILAC)

Figure 2.11: The Ion Sources

2.4.13 Visit of FAIR Construction Site

Access to the construction area was strictly controlled, requiring all visitors to adhere to rigorous safety protocols. Prior to entry, participants were required to pass a safety procedure test and don the necessary personal protective equipment, including safety shoes, high-visibility vests, and hard hats (2.12). The visit provided a unique opportunity to walk through sections of the newly constructed accelerator tunnels. The machinery visible within the tunnel (2.13) is identified as components of the SIS100.

2.5 Activities

2.5.1 Pedestrian rally in Darmstadt

The Pedestrian Rally in Darmstadt was one of the first social events, typically held during the program's initial week. This activity served as an engaging way

Figure 2.12: The personal protective equipment

Figure 2.13: The SIS100 accelerator

for students to explore the city of Darmstadt while simultaneously fostering a collaborative environment. Participants were divided into small teams to complete game-based challenges and tasks across key city landmarks. This event was highly effective in breaking the ice and promoting early relationship-building among the international group of students, while also providing a valuable introduction to the history and culture of the host city.

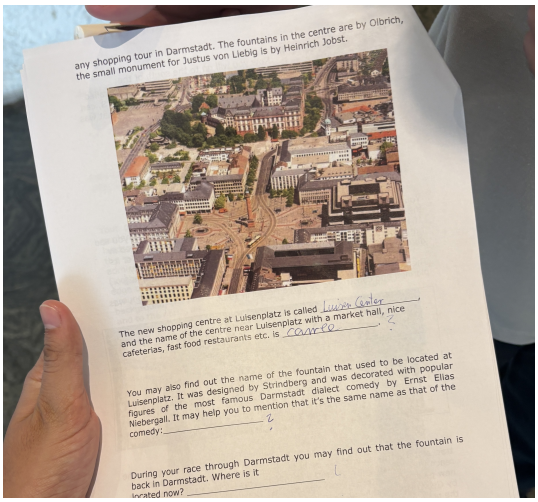

Figure 2.14: Pedestrian rally in Darmstadt

2.5.2 BBQ Grill and Chill Party

The BBQ Grill and Chill Party was a significant social event designed to foster cultural exchange and networking among the international students and researchers. Students utilized the facility's available space, which could be reserved for hosting parties, to organize a shared barbecue. The atmosphere promoted informal conversation and the exchange of knowledge and cultural perspectives

among the participants (2.15). This event was highly effective in building camaraderie outside of the academic context.

Figure 2.15: BBQ Grill and Chill Party

2.5.3 Ioni Summer Cup: Sports Fun Event

The Ioni Summer Cup was organized by the GSI Sports Club as a large-scale Sport Fun Event, inviting both Summer Students and GSI staff members, including tutors. This event facilitated interaction between the international students and the GSI personnel through organized sports competitions and various group activities. Following the daytime sporting events, the evening featured a concert performed by GSI staff members, which included dancing and further social engagement, successfully fostering collaboration and community building across the academic and staff sectors.

Figure 2.16: Ioni Summer Cup: Sports Fun Event

2.5.4 Annual Workshop & Grill and Chill

The GSI-FAIR Annual Workshop successfully combined academic exchange with social networking. The event featured facility tours and dedicated group discussions, fostering vital knowledge exchange among international students and researchers (2.17). A key highlight was the physical demonstration of crucial infrastructure components, such as the Silicon Target (2.18), providing a tangible link to the CBM experiment at FAIR. The workshop concluded with a Grill and Chill party, promoting community building outside the laboratory setting.

Figure 2.17: Grill and Chill party

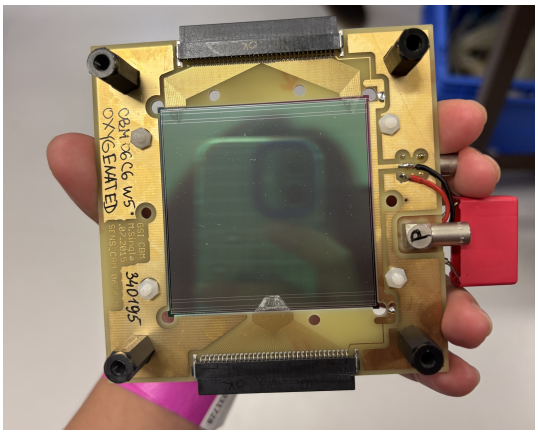

Figure 2.18: The Silicon Target

Chapter 3

Research Overview

Students are required to submit their individual research reports developed during the program by Week 7. They should then prepare to present their work the following week. All reports are compiled into a bound book, with every participant receiving two physical copies. Participants generally keep one copy and hand the other to their assigned tutor. Crucially, neither the individual reports nor the compiled project book have been published online. For this reason, the Thai representative has included their complete report in the Appendix, along with a concise summary of the research findings, which is detailed below:

Charmed Exotica at SIS 100 Energies

3.1 Background and Motivation

The research is motivated by the global focus on studying new and exotic hadronic states in hadron physics. The FAIR heavy ion research facility is under development, and the PANDA experiment there was initially designed to contribute to these studies by using anti-proton and proton collisions to produce the hadrons of interest.

However, due to a delay in the PANDA experiment, a new strategy emerged: utilize the CBM experiment known for its high data-rate capabilities to investigate some of these exotic hadrons instead.

The primary goal of this work was to establish estimates for the production of Exotic charmed states (like charmed hadrons and charmed nuclei) and Charm production rates in heavy ion (Au+Au) and proton-ion (p+Au) reactions at the CBM experiment's SIS100 energy level.

These predictions are highly relevant because they provide crucial input for upcoming experiments at FAIR and GSI. Observing charm and exotic bound states in these extreme conditions would yield valuable information about Quantum Chromodynamics (QCD). Furthermore, the research included a comparison of these rates to the much higher production rates expected and measured at the LHC, which helps in understanding how charm production differs between low- and high-energy systems.

3.2 Objectives

1. To predict the production of charmed hadrons and charmed nuclei within the framework of the Statistical Hadronization Model (SHM).

2. To evaluate the production yield of exotic particles in heavy-ion and proton-nucleus collisions (Au+Au and p+Au) at SIS100 energies.

3. To compare this production with the maximum energy data at the LHC (Pb+Pb at 5.02 TeV) to understand the differences between low and high-energy systems in charm production.

3.3 Related Theories

3.3.1 Charm Quarks in High-Energy Collisions

In the extreme conditions created by high-energy nuclear collisions, the dynamics of charm quarks(c) are crucial for probing the properties of the strongly interacting matter known as the **Quark-Gluon Plasma (QGP)**. Charm quarks are classified as heavy quarks, possessing a mass of approximately $m_c \approx 1.27\ GeV/c^2$. They are predominantly produced during the early stages of the collision, and their total number is generally assumed to be conserved throughout the subsequent evolution of the **fireball**.

The subsequent distribution of these conserved charm quarks into various hadronic states (a process known as hadronization) occurs at the point of chemical freeze-out. This final distribution provides critical insights into the thermal and chemical properties of the system.

The strong interaction is governed by Quantum Chromodynamics (QCD), which fundamentally describes the behavior of quarks and gluons. QCD predicts two key phenomena: asymptotic freedom at high energies (where quarks and gluons interact weakly) and color confinement at low energies (where quarks are bound into hadrons).

Charm hadrons, which are particles containing at least one charm quark, can be broadly categorized into four groups:

1. Open Charm Mesons: Such as the D and D^* mesons.

2. Charmed Baryons: Including Λ_c and Σ_c.

3. Hidden Charm States (Charmonia): Where the total charm quantum number is zero, such as the J/ψ and ψ mesons.

4. Exotic States: Non-conventional quark-gluon configurations, including tetraquarks, pentaquarks, and bound states of charmonium with atomic nuclei.

3.3.2 The Statistical Hadronization Model (SHM)

The SHM serves as a robust theoretical framework for approximating the production probability of diverse hadrons in high-energy collisions. The model posits that the energetic matter created by the collision (often referred to as a **cluster** or **fireball**) decouples into a final state of hadrons in a purely statistical manner.

The central tenet of the SHM is that every multi-hadronic state is equally probable, provided it adheres to fundamental conservation laws. Consequently, the relative abundances of all produced hadrons are governed by a small set of **thermal** parameters, primarily the Temperature (T) and the associated chemical potentials (μ).

The model has been remarkably successful in accurately describing particle yields in both large systems, like heavy-ion collisions, and smaller systems, such as elementary collisions. Furthermore, the SHM has been shown to successfully predict the relative charm hadron abundances using the same thermal parameters, provided the initial total number of charm quarks is fixed.

3.3.2.1 Canonical Ensemble and Hadron Multiplicity

In the SHM, hadron yields are calculated from the system's partition function. While the Grand-Canonical Ensemble is typically used for large systems where conserved charges (like baryon number, strangeness, and charm) are conserved only on average this approximation breaks down for small or intermediate systems.

For these smaller systems, the exact conservation of charges is mandatory, requiring the use of the **Canonical Ensemble**. The Canonical Partition Function, Z(**Q**), for a system with conserved charges **Q**, is derived as a projection of the Grand-Canonical Partition Function onto fixed values of these charges.

$$\begin{aligned} Z(\mathbf{Q}) = & \frac{1}{(2\pi)^N} \int_{-\pi}^{+\pi} d^N\phi \, e^{i\mathbf{Q}\cdot\phi} \quad \times \exp\left[\frac{V}{(2\pi)^3} \sum_j (2S_j+1) \right. \\ & \left. \int d^3p \, \log\left(1 \pm \gamma_s^{N_{sj}} e^{-\sqrt{p^2+m_j^2}/T_i - i\mathbf{q}_j\cdot\phi}\right)^{\pm 1} \right] \end{aligned} \tag{3.1}$$

The calculation of the **primary multiplicity** $\langle n_j \rangle^{primary}$ (the number of hadrons of species j produced directly from the fireball) is directly determined by this Canonical Partition Function. This calculation depends on the system's thermal properties (Volume V and Temperature T of the Equivalent Global Cluster, or

EGC) and the hadron's intrinsic properties (mass m_j and spin S_j). A phenomenological parameter, $\gamma_S$is often included to account for the observed suppression of strange hadrons.

$$\langle n_j \rangle^{primary} = \frac{VT(2S_j+1)}{2\pi^2} \sum_{n=1}^{\infty} \gamma_S^{N_s n} (\mp 1)^{n+1} \times \frac{m_j^2}{n} K_2\Big(\frac{nm_j}{T}\Big) \frac{Z(\mathbf{Q}-nq_j)}{Z(\mathbf{Q})}$$

Finally, to allow for direct comparison with experimental measurements, the total hadron multiplicity is computed by adding the contributions from the decay of unstable, heavier hadrons to the primary yield:

$$\langle n_j \rangle^{total} = \langle n_i \rangle^{primary} + \sum_k (k \to j) \langle n_k \rangle \tag{3.2}$$

This comprehensive approach allows the SHM to connect the fundamental concepts of QCD and thermodynamics to the experimentally observable yields of both known and exotic charmed particles.

3.4 Results and discussion

3.4.1 Determining Input Parameters for the SHM

To accurately predict the multiplicities of charmed hadrons and nuclei at SIS100 energies using the Statistical Hadronization Model (SHM), The freeze-out parameters (T and μ_B) are required as crucial input.

Furthermore, applying the charm-canonical approach of the SHM necessitates two independent charm hadron multiplicities to constrain the total number of charm quarks and the canonical radius. Since direct experimental data is unavailable for SIS100 energies, these essential inputs must be derived from reliable model simulations.

For this work, we employed the UrQMD model (version v4.0), a code well-established for describing various hadron multiplicities. This specific version has also been extended to provide predictions for charm production within the SIS100 energy range.

3.4.2 Model-Based Input Multiplicities

The UrQMD model was used to simulate particle multiplicities for Au+Au collisions at SIS100 energies, covering six different center-of-mass energies: 2.4, 3.0, 3.5, 4.0, 4.5, and 5.0 GeV. The simulations were grouped into four distinct

centrality classes: 0-10%, 10-20%, 20-30%, and 30-40%.

The specific hadron multiplicities extracted from these UrQMD simulations include:

- Light-flavor hadrons: π^+, π^-, K^+, K^-, p, $\bar{p}$, Λ, $\bar{\Lambda}$, Ξ^-, Ω, and K^0_S.
- Charmed hadrons: J/ψ and Λ_c

3.4.3 Thermal Parameter Extraction

These obtained multiplicities were subsequently analyzed within the framework of the (charm-canonical) Statistical Hadronization Model using the Thermal-FIST program. This fitting procedure allowed us to extract the key thermal parameters for each specific centrality class and energy point: the chemical freeze-out temperature (T) and the baryon chemical potential (μ_B). The resulting fitted parameters are graphically represented in Figure 3.1

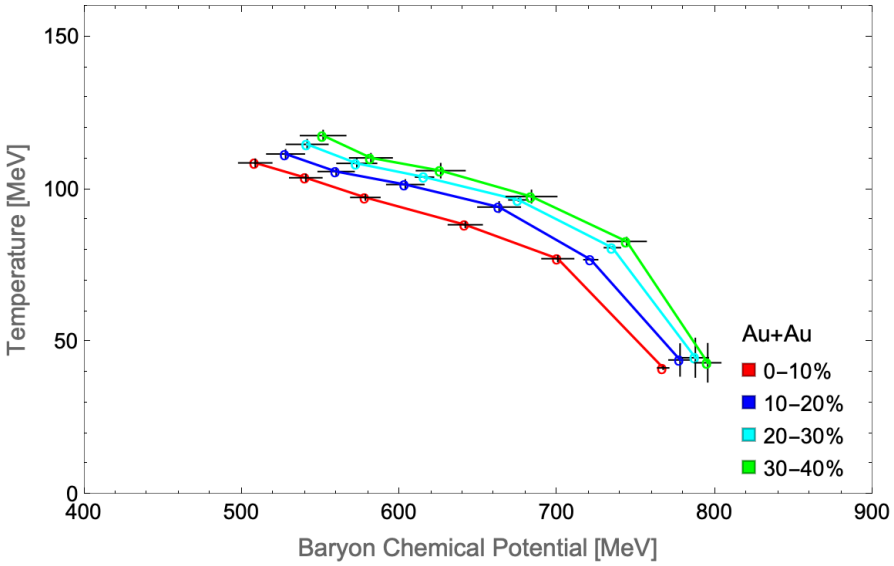

Figure 3.1: Chemical freeze out Temperatures and Baryon Chemical Potentials for Au+Au collisions at different centralities.

The plot clearly demonstrates the inverse relationship between T and μ_B (Figure 1): as collision energy decreases, the $\mu_B$of the system increases, while the corresponding T drops notably. This observation aligns with the expected behavior of the phase boundary in the QCD phase diagram as it moves toward higher net-baryon densities.

When examining the different centrality classes, a subtle centrality dependence on T is observed. For a given μ_B, the more peripheral collisions generally exhibit slightly higher temperatures compared to the most central collisions. Despite this

minor variance, the overarching, inverse relationship between T and μ_B remains robust across all measured centrality classes.

3.4.4 Predicted Particle Multiplicities

We now proceed to the core objective: predicting particle multiplicities. For clarity in presenting the results, we have categorized the particles whose multiplicities we intend to predict into four distinct groups. The subsequent figures will illustrate the relationship between the predicted Multiplicity of each particle type and the center-of-mass energy ($\sqrt{s_{NN}}$) across the SIS100 energy range.

The four categories of predicted particle multiplicities are:

1. Normal Hadrons: π^+, K^+, K^-, p, $\bar{p}$, Λ, Ξ^-, d, t, and Ω.
2. Charms: J/ψ, Λ_c, D_0, and $\bar{D}_0$
3. Exotics: $X(3872)$, D_s, η_c, $\chi_{c0}(1P)$, $\chi_{c1}(1P)$, $\Sigma_c^+(2455)$, and $\Sigma_c^{++}(2455)$.
4. Nuclei: $\{pn\Lambda_c\}$, $\{n\Lambda_c\}$, $\{pnn\Lambda_c\}$, and $\{\alpha D^-\}$.

A number of exotic charmed hadrons and nuclei were not readily available in the default particle database of the Thermal-FIST software. To facilitate predictions for these species, they were manually appended to the particle list by precisely defining their fundamental quantum numbers, including their mass, charge, baryon number, strangeness, charm, and the absolute value of the charm quantum number ($|C|$).

Particle	Mass[GeV]	Q	B	S	C	$\|C\|$
$\{\mathrm{pn}\Lambda_c\}$	4.163	2	3	0	1	1
$\{\mathrm{n}\Lambda_c\}$	3.225	1	2	0	1	1
$\{\mathrm{pnn}\Lambda_c\}$	5.102	2	4	0	1	1
$\{\alpha D^-\}$	5.596	1	4	0	-1	1
X(3872)	3.872	0	0	0	0	2
D_s^+	1.968	1	0	1	1	1
$\eta_c(1S)$	2.984	0	0	0	0	2
$\chi_{c0}(1P)$	3.414	0	0	0	0	2
$\chi_{c1}(1P)$	3.510	0	0	0	0	2
Σ_c^{++}	2.454	2	1	0	1	1
Σ_c^+	2.453	1	1	0	1	1

Table 3.1: List of charmed hadrons and nuclei that have been introduced to thermal-FIST with their masses and quantum numbers.

3.4.4.1 Normal Hadron Multiplicities

Figure 3.2 presents the predicted multiplicities for Normal Hadrons (lines) compared to the input values obtained from UrQMD simulations (symbols) across the SIS100 energy range. The data is separated into four centrality classes.

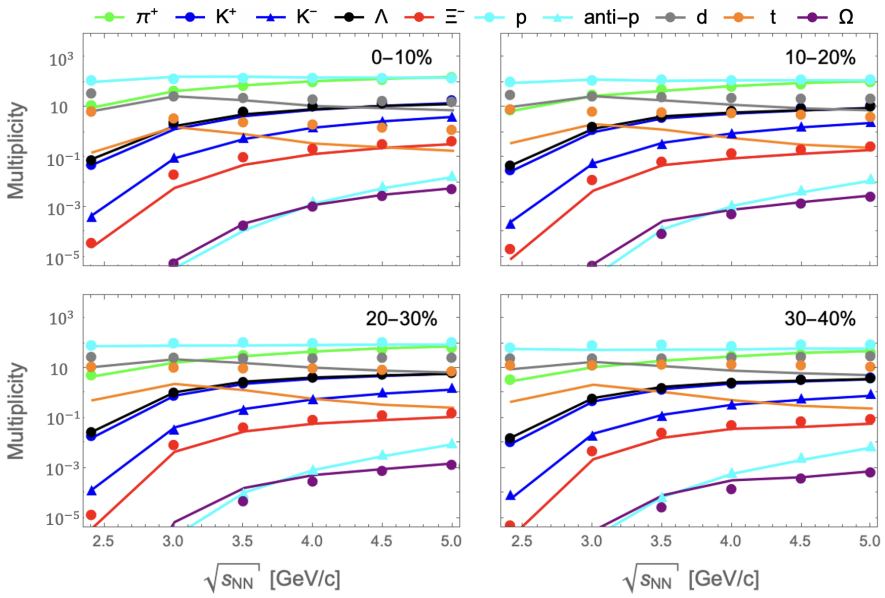

Figure 3.2: Predicted(lines) and Input(markers) normal hadron multiplicities in Au+Au collisions.

The SHM prediction (lines) demonstrates a strong overall agreement with the UrQMD input (symbols) for most of the studied light-flavor particles (π^+, K^+, K^-, p, $\bar{p}$, Λ, Ξ^-, Ω) This consistency validates the extracted thermal parameters T and μ_B and confirms that the canonical Statistical Hadronization Model provides a reliable description of light-hadron production within the SIS100 energy regime.

However, notable discrepancies are observed for two specific species: the deuteron (d) and the triton (t). For these two light nuclei, the SHM predictions (lines) show a clear deviation from the UrQMD input values (symbols), particularly at lower center-of-mass energies. This lack of agreement is expected, as d and t were not included in the initial set of hadron multiplicities used to constrain the thermal parameters during the fitting process (the primary input for the fit focused on single-baryon and meson species).

3.4.4.2 Charm Multiplicities

Figure 3.3 illustrates the predicted multiplicities of several key charm hadrons J/ψ, Λ_c, D_0, and $\bar{D}_0$ as a function of center-of-mass energy ($\sqrt{s_{NN}}$) across four centrality classes.

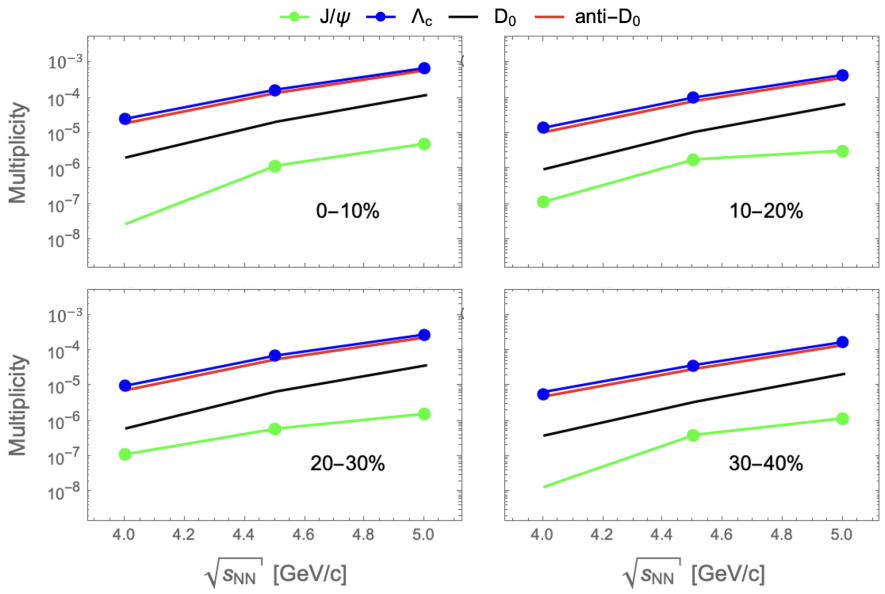

Figure 3.3: Predicted(lines) and Input(markers) charm multiplicities in Au+Au collisions.

Across all measured energies and centrality classes, the Hidden Charm state (J/ψ) exhibits the lowest multiplicity, trailing the Open Charm states (Λ_c, D_0, $\bar{D}_0$) by several orders of magnitude.

This observed hierarchy is physically well-justified by the respective quark content of the particles:

1. Open Charm Hadrons (Λ_c, D_0, and $\bar{D}_0$): These particles each contain only one charm quark (or anti-charm quark) paired with lighter quarks ($\Lambda_c = udc$, $D_0 = c\bar{u}$). Their formation relies on the initial production of a single $c\bar{c}$ pair, followed by the combination of the charm quark with light thermal quarks from the bulk medium. Since c quarks are conserved, the overall production rate of these single-charm particles is higher.

2. Hidden Charm Hadrons (J/ψ): The J/ψ is a charmonium state ($c\bar{c}$). Its formation requires the recombination of the initially produced charm quark and the anti-charm quark into a bound state at freeze-out. This requirement imposes a more stringent constraint, naturally leading to a significantly lower overall multiplicity compared to the single-charm states.

The multiplicities for all charm hadron species are observed to be rising with increasing center-of-mass energy ($\sqrt{s_{NN}}$). This general trend reflects the fact that higher collision energies lead to a greater total production of $c\bar{c}$ pairs in the initial stage of the collision. The relative abundances, however, remain consistent across the studied centrality bins, reinforcing the robustness of the SHM's thermal approach to charm hadronization.

3.4.4.3 Exotic Multiplicities

Figure 3.4 displays the predicted multiplicities for a selection of higher-mass and less-common charm states, including X(3872) (which is set as a high-mass charmonium $c\bar{c}$ state in this analysis), D_s, η_c, $\chi_{c0}(1P)$, $\chi_{c1}(1P)$, and Σ_c baryons. The results are shown as a function of center-of-mass energy ($\sqrt{s_{NN}}$) across the four centrality classes.

A primary observation from this plot is the clear inverse relationship between the particle mass and its predicted multiplicity. This is a direct consequence of the thermal nature of the SHM, where production is suppressed exponentially by mass ($e^{-m/T}$). Generally, heavier charm states are produced less frequently.

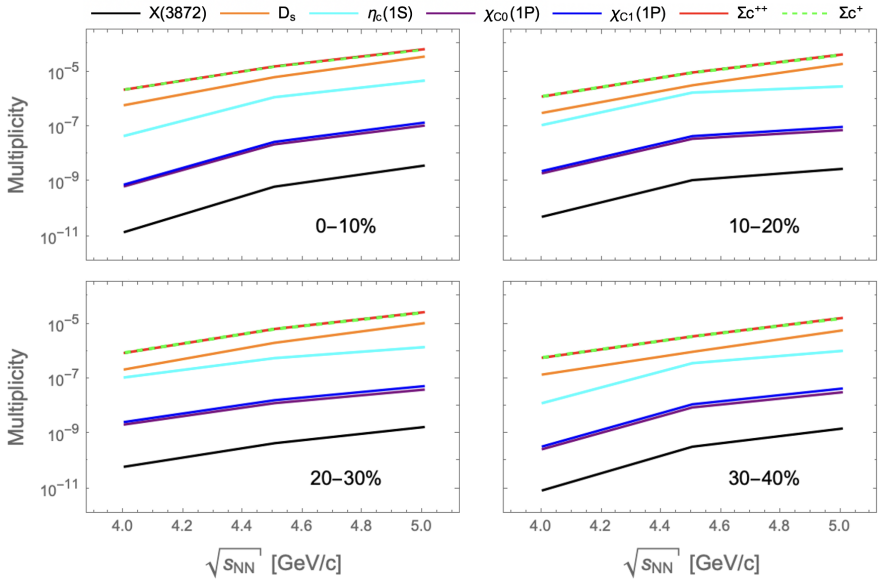

Figure 3.4: Predicted(lines) and Input(markers) exotic multiplicities in Au+Au collisions.

The hierarchy of production rates reflects this mass dependence and the particle structure:

1. Higher Yields: Open-charm states, such as the $D_s$meson and the Σ_c baryons, exhibit the highest multiplicities in this group, consistent with their relatively lower mass and single-charm content.

2. The $X(3872)$ state, set here as the heaviest charmonium state, exhibits the lowest predicted multiplicity among all species in this figure. This result is entirely consistent with the thermal framework, as its very high mass imposes the strongest thermal suppression factor, placing it at the bottom of the production hierarchy.

Based on the consistent result that the $\Lambda_c$baryon maintains the highest predicted multiplicity among all single-charm hadrons analyzed, it was selected as the representative species for the upcoming stages of analysis.

Specifically, the high production rate of the Λ_c makes it the critical input for investigating the thermal production Nuclei, the results of which are presented in Figure 3.5. Furthermore, the Λ_c multiplicity will be used to investigate the dependence of particle multiplicity on the Baryon Number (B), which is the focus of Figure 3.6.

3.4.4.4 Nuclei Multiplicities

Figure 3.5 illustrates the predicted multiplicities for various Charmed Nuclei (bound states containing a Λ_c baryon or an anti-D meson) as a function of center-of-mass energy ($\sqrt{s_{NN}}$).

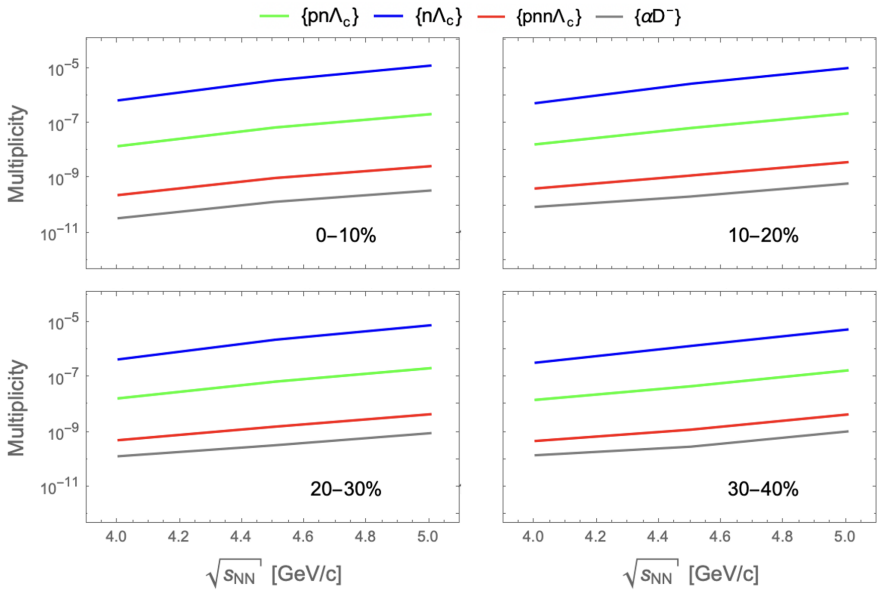

Figure 3.5: Predicted(lines) and Input(markers) nuclei multiplicities in Au+Au collisions.

This result provides critical insight into the dynamics of forming these exotic bound states at chemical freeze-out:

1. The $\{n\Lambda_c\}$ state exhibits the highest production rate, which is physically justified by its composition as the simplest (two-body) Charmed Nucleus in this study.

2. The hierarchy generally confirms the dominant role of thermal mass suppression. As the complexity and overall mass of the bound state increases (moving from $\{n\Lambda_c\}$ to the three-body state $\{pn\Lambda_c\}$ and then to the heavier four-body states), the production yield decreases exponentially ($e^{-m/T}$).

3.4.5 Particle Multiplicity vs. Baryon Number

Figure 3.6 displays the multiplicity of charmed nuclei as a function of the baryon number (B). The data includes results from three SIS100 beam energies (4.0 GeV,4.5 GeV, and 5.0 GeV), represented by blue, red, and green symbols, respectively. The plot also incorporates predicted yields based on ALICE experimental data from Pb+Pb collisions at 5.02 TeV (LHC), represented by black symbols.

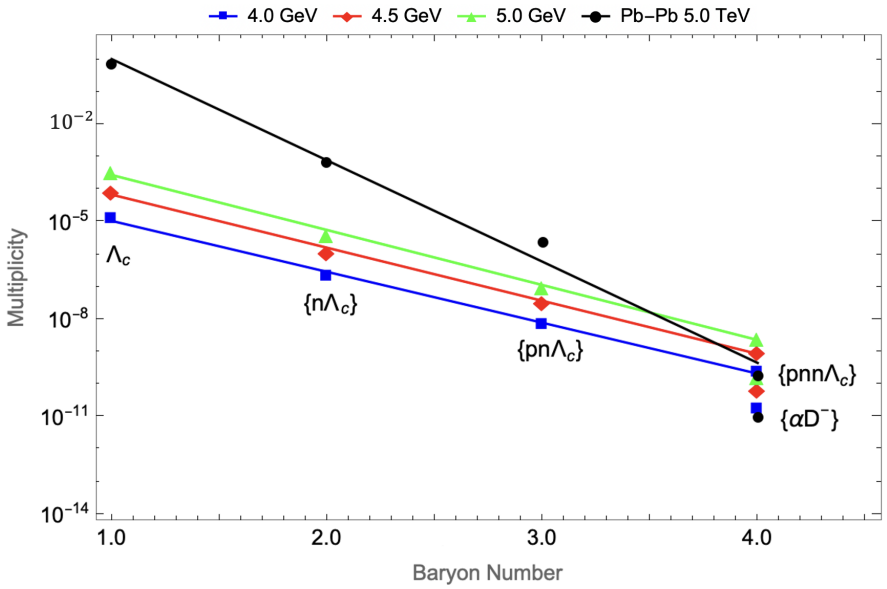

Figure 3.6: Particle multiplicities as a function of Baryon Number for Au+Au and Pb+Pb collisions.

Initially, the expected hierarchy is clear: the production of the single-baryon $\Lambda_c(B = 1)$ is significantly higher in LHC Pb+Pb collisions than in SIS100 Au+Au collisions. This is due to the much larger size of the colliding system (Pb+Pb vs. Au+Au) and the substantially higher collision energy at the LHC, which drastically increases the initial charm production probability.

However, the key and most interesting observation emerges as the baryon number increases:

- As the states become heavier and more complex ($B = 3$ and 4), the production yields in the SIS100 Au+Au system begin to approach and eventually surpass the yields predicted for the LHC Pb+Pb system.
- For the heaviest B=4 nuclei ($\{pnn\Lambda_c\}$ and $\{\alpha D^-\}$), the Au+Au multiplicities are observed to be higher than the LHC values.

This crossover phenomenon demonstrates that the high baryon chemical potential (μ_B) prevalent at lower SIS100 energies effectively boosts the thermal pro-

duction of heavy multi-baryon states. The high density of thermal baryons compensates for the strong thermal mass suppression, making SIS100 an unexpectedly favorable environment for studying the production of these heaviest charmed nuclei, even compared to the high-energy LHC environment.

3.4.6 Comparison with Other Systems

In addition to the primary focus on Au+Au collisions at SIS100 energies, the present work extends the analysis to compare charm and exotic production across different collision systems and at at higher energies.

Particle	Au+Au	p+Au	Pb+Pb
$\{pn\Lambda_c\}$	2.153×10^{-7}	7.171×10^{-8}	4.910×10^{-6}
$\{n\Lambda_c\}$	1.256×10^{-5}	1.119×10^{-6}	0.002
$\{pnn\Lambda_c\}$	2.761×10^{-9}	3.510×10^{-9}	1.932×10^{-10}
$\{\alpha D^-\}$	3.597×10^{-10}	1.809×10^{-9}	1.867×10^{-11}
X(3872)	3.805×10^{-9}	4.509×10^{-8}	0.001
D_s^+	3.566×10^{-5}	5.489×10^{-7}	2.905
$\eta_c(1S)$	4.755×10^{-6}	9.242×10^{-6}	0.132
$\chi_{c0}(1P)$	1.092×10^{-7}	5.118×10^{-7}	0.010
$\chi_{c1}(1P)$	1.403×10^{-7}	7.931×10^{-7}	0.016
Σ_c^{++}	6.655×10^{-5}	2.167×10^{-6}	0.159
Σ_c^+	6.395×10^{-5}	2.065×10^{-6}	0.134

Table 3.2: Predicted particle multiplicities in central Au+Au ($\sqrt{s_{NN}} = 5.0$ GeV), p+Au ($\sqrt{s_{NN}} = 5.62$ GeV), and central Pb+Pb collisions ($\sqrt{s_{NN}} = 5.02$ TeV).

3.4.6.1 Proton-Gold (p+Au) Collisions

The investigation includes predictions for p+Au collisions at $\sqrt{s_{NN}} = 5.62$ GeV. Although this is a smaller system, utilizing the 0–10% centrality selection allows for a meaningful comparison with heavy-ion systems.

The predicted multiplicities for this system are summarized in Table 3.2. Table 3.2 also lists the multiplicities expected in p+Au collisions at the SIS100 energy range, which is slightly above the elementary charm production threshold. As can be observed from the data, the overall charm production probability is significantly increased compared to the sub-threshold energies previously discussed.

3.4.6.2 Pb+Pb Collisions at LHC Energy

Following the analysis of the exponential suppression of charmed nuclei yields in Figure 3.6, we now utilize Table 3.2 to present the precise numerical yields and highlight the significant differences between collision systems.

To establish an experimental benchmark for the ultra-high-energy regime, we utilize available experimental data from the ALICE collaboration on hadron and charm production in central Pb+Pb collisions at $\sqrt{s_{NN}} = 5.02\ TeV$ (including yields for J/ψ, Λ_c, D mesons, and D_s). By utilizing the corresponding chemical freeze-out temperature of $T_c = 156\ MeV$ derived from this experimental data, we are able to successfully predict the yields of exotic states for the LHC energy regime within the Statistical Hadronization Model (SHM).

This comparative analysis is essential because while the figure shows the trend, Table 3.2 provides the critical numerical evidence that, for the heaviest multi-baryon states ($B = 4$), the production yield at the SIS100 (high μ_B) becomes comparable to, or even surpasses, the yield predicted for the LHC (low μ_B) system.

3.4.7 Conclusion

In this work, we successfully utilized the Statistical Hadronization Model (SHM), parameterized by chemical freeze-out temperature (T) and baryon chemical potential (μ_B), to predict the production yields of charmed hadrons and exotic charmed nuclei in heavy-ion (Au+Au) and proton-ion (p+Au) collisions at SIS100 energies, and provided a comparative benchmark with the LHC regime.

The key findings are summarized as follows. First, regarding Mass and Baryon Number Suppression: the predicted multiplicities for all charm species from normal to exotic hadrons and charmed nuclei exhibit the expected exponential suppression with increasing mass and baryon number, a characteristic feature of thermal production.

Second, concerning LHC vs. SIS100 Yields: as anticipated, the overall production rate of charm is significantly higher (by several orders of magnitude) at the LHC ($\sqrt{s_{NN}} = 5.02\ TeV$) compared to the SIS100 energies. This is primarily due to the strong suppression of sub-threshold charm production at lower energies.

Despite the lower overall charm production at SIS100, a crucial and non-trivial result was found: for the heaviest multi-baryon states (specifically the B = 4 charmed nuclei), the production yield predicted for the Au+Au collisions at SIS100 (high μ_B) becomes comparable to, or even exceeds, the yield predicted for the Pb+Pb collisions at the LHC.

This crossover demonstrates that the high baryon chemical potential prevalent at SIS100 effectively compensates for the thermal mass suppression. This makes experiments like CBM@FAIR an unexpectedly favorable environment for the synthesis and future detection of these heavy exotic states.

Chapter 4

Experiences

4.1 Cycling Culture

Daily life during the program was largely centered around effective transportation between the accommodation and the GSI campus, which was situated approximately four kilometers away. Bicycles quickly became the primary mode of transport for the majority of the summer students. This experience provided an unexpected but valuable opportunity to learn and adapt to the specific cycling laws and regulations enforced on public roads in Germany. Navigating the city and commuting by bicycle not only supported daily logistics but also offered a practical way to integrate into the local culture and environment outside of the research facility.

Figure 4.1: Daily life during the program with bicycle

4.2 Excursion to Frankfurt

A highlight of the social experience was a weekend excursion to Frankfurt, where the author had the opportunity to visit significant city landmarks. This trip was particularly enriching as it was undertaken with Postdoctoral Researchers, providing insights not only into German culture and history but also into the

lifestyle of senior researchers. The process of traveling and living in Germany further involved practical cultural adjustments, notably the daily reliance on the Euro currency. These trips served to broaden the overall international experience, transitioning from the technical environment of the lab to understanding the broader social and financial landscape of the host country.

Figure 4.2: The Euro currency landmark in Frankfurt

4.3 Excursion to Bonn and Hiking the Löwenburg

The cultural experience was further enriched by an excursion to the city of Bonn, the former capital of West Germany. The trip's highlight was a scenic hiking trip to the Löwenburg (Lion's Castle), located in the Siebengebirge Nature Park. This activity provided a welcome break from the intense research schedule, allowing for physical activity and appreciation of the natural German landscape. The outing demonstrated the accessibility of significant natural and historical sites across the region and offered another opportunity for casual social bonding with fellow program participants outside of the formal research setting.

4.4 Hiking to Frankenstein Castle

Another memorable outing involved a hike to the historic Frankenstein Castle, a well-known landmark near Darmstadt. This excursion provided both physical activity and a rich connection to local folklore and history. The journey involved navigating scenic trails leading up to the castle ruins. This activity served as an excellent opportunity for the students to bond socially while exploring the

Figure 4.3: Hiking the Löwenburg

region's historical sites, offering a refreshing contrast to the high-tech, theoretical environment of GSI.

Figure 4.4: Hiking to Frankenstein Castle

4.5 Relaxing by the River

Beyond the organized social events, much of the valuable cultural exchange occurred during informal gatherings. A notable leisure activity involved spending afternoons by the river, engaging in card games with European peers. These casual sessions provided a relaxed atmosphere for open dialogue, facilitating a deeper social and cultural bond among the international students. These moments were essential for transitioning beyond professional relationships and fostering lasting personal connections.

Figure 4.5: The Main River in Frankfurt.

4.6 Farewell Meals and Culinary Exchange

During the final week before departure, the living situation fostered a strong sense of community and generosity. Food expenses were significantly reduced as departing students left behind a substantial amount of unused groceries and cooking ingredients for those remaining. This abundance led to collective cooking and communal meals, which became a delightful opportunity for final cultural and culinary exchange. The author specifically had the chance to prepare and share Ramen with a roommate, serving as a memorable farewell gesture before returning home. This shared experience highlighted the strong bonds formed throughout the eight weeks.

Figure 4.6: My roommate

Figure 4.7: The plenty of food

4.7 Photo with My tutor

Figure 4.8: My tutor is in the middle

Chapter 5

Appendix

Charmed Exotica at SIS100 energies

Thanaporn Chimruang
Suranaree University of Technology, thanaporn6516@gmail.com

In this work, we investigate the production of charmed hadrons and nuclei within the statistical hadronization framework. The goal is to predict the expected production multiplicities of these exotic hadronic states at the planned SIS100 accelerator and compare them to expected rates at the highest available energies at the LHC. At FAIR/SIS100 energies (Au+Au collisions at 4.0–5.0 GeV), the predicted yields of exotic states are found to be several orders of magnitude lower than those observed in Pb+Pb collisions at 5.02 TeV by ALICE. However, due to the expected high luminosity at the SIS100 the measurement of some of these states may still be feasible. Escpecially the production of charmed nuclei is as likely as at the LHC due to the large number of baryons present at chemical freezeout.

1 Introduction

The exploration of new and exotic hadronic states has been the focus of hadron physics programs around the world. The PANDA experiment at FAIR was planned to contribute to these studies through the collisions of antiprotons and protons which could produce many of the hadrons of interest. Due to the delay of PANDA a new idea has emerged to use the CBM experiment and its high data-rate capabilities to study some of these exotic hadrons. The goal of this work was to establish estimates on the production of exotic charmed states and charmed nuclei in heavy ion and proton-ion reactions at the CBM experiment.

In addition, we compared those rates to expectations for experiments at the LHC where much higher charm production rates are expected and have been measured. Within the statistical hadronization model (SHM) the production yields and relative abundances of charm hadrons, including open charm mesons, charmed baryons, hidden charm states, and possible exotic configurations have been estimated. Such predictions are highly relevant for upcoming experiments at FAIR and GSI, where the observation of charm and exotic bound states would provide valuable information on QCD in extreme conditions.

2 Background

In high-energy nuclear collisions, charm quarks are produced in the early stage and the total number of charm quarks is thought to be conserved throughout the evolution of the fireball. Their distribution into various hadrons occurs at chemical freeze-out and provides important insight into the properties of strongly interacting matter.

In principle, the production of charm hadrons in relativistic heavy-ion collisions can be described in the theoretical framework of Quantum Chromodynamics (QCD), the fundamental theory of the strong interaction. QCD describes the dynamics of quarks and gluons, and it predicts two essential features: asymptotic freedom at high energies and color confinement at low energies.

In QCD, the charm quark with a mass of about 1.27 GeV/c^2, belongs to the family of heavy quarks. Charm hadrons can be broadly categorized as:

1. Open charm mesons, such as D and D^*,
2. Charmed baryons, such as Λ_c and Σ_c,
3. Hidden charm states, including the J/ψ and ψ mesons,
4. Exotic states, such as tetraquarks, pentaquarks, or bound states of charmonium with nuclei.

2.1 The Statistical Hadronization Model (SHM)

The Statistical Hadronization Model (SHM) (see [1] and references therein) is a model used to approximate the production probability of different hadrons in high-energy particle collisions. The central idea of this model is that at the end of a collision, the resulting energy and matter forms massive, colorless objects called clusters or fireballs. These clusters then decays into a final state of hadrons in a purely statistical manner. The core principle of the SHM is that every possible multi-hadronic state within a cluster, as long as it respects conservation laws, is equally likely. Consequently the relative abundances of hadrons in any such collision can be characterized by its thermal parameters Temperature (T) and chemical potentials (μ).

The SHM provides a surprisingly accurate description of particle yields in both heavy ion collisions and even simpler, elementary collisions. It was even shown that, once the initial number of charmed quarks is fixed, the SHM can accurately predict the relative abundances of charm production with the same parameters [2]

2.2 Canonical Partition Function

In the Statistical Hadronization Model (SHM), the multiplicities of hadrons are computed from the partition function of the system. In large systems, one often employs the grand-canonical ensemble, where conserved charges such as baryon number, strangeness, or charm are only conserved on average through associated chemical potentials.

However, in small or intermediate systems such as those created in elementary collisions, this approximation breaks down. In such cases, an exact conservation of charges is required, and the canonical ensemble must be used. The canonical partition function $Z(\mathbf{Q})$ [1] for a system with conserved charges $\mathbf{Q}$ can be expressed as a projection of the grand-canonical partition function onto fixed values of these charges. A common representation is given by Equation 1:

$$Z(\mathbf{Q}) = \frac{1}{(2\pi)^N} \int_{-\pi}^{+\pi} d^N\phi \, e^{i\mathbf{Q}\cdot\phi} \times \exp\left[\frac{V}{(2\pi)^3} \sum_j (2S_j+1) \int d^3p \, \log\left(1 \pm \gamma_s^{N_{sj}} e^{-\sqrt{p^2+m_j^2}/T_i - i\mathbf{q}_j\cdot\phi}\right)^{\pm 1}\right] \quad (1)$$

This integral formulation ensures the exact conservation of charges, a crucial feature for accurately describing small systems.

The primary multiplicity, or the number of hadrons of a specific species j produced directly from the hadronization process, is determined by the canonical partition function. The expression for the primary multiplicity (2)

$$\langle n_j \rangle^{primary} = \frac{VT(2S_j+1)}{2\pi^2} \sum_{n=1}^{\infty} \gamma_S^{N_s n} (\mp 1)^{n+1} \times \frac{m_j^2}{n} K_2\Big(\frac{nm_j}{T}\Big) \frac{Z(\mathbf{Q}-nq_j)}{Z(\mathbf{Q})} \quad (2)$$

where V and T are the volume and temperature of the Equivalent Global Cluster (EGC). m_j and S_j are the mass and spin of hadron j. γ_S is a phenomenological parameter introduced to account for the observed suppression of strange hadrons.

Finally, to obtain the total number of hadrons that can be directly compared with experimental data, the contributions from the decay of unstable, heavier hadrons must be added. This is represented by Equation 3:

$$\langle n_j \rangle^{total} = \langle n_i \rangle^{primary} + \sum_k (k \to j) \langle n_k \rangle \quad (3)$$

3 Results

Using the SHM, in order to predict the multiplicities of charmed hadrons and nuclei at SIS100 we require the corresponding temperatures and chemical potentials as input. In addition, to constrain the total number of charm and its canonical radius, two independent charm hadron multiplicities are necessary as input. Since no experimental measurements for the SIS100 exist, this input will come from model

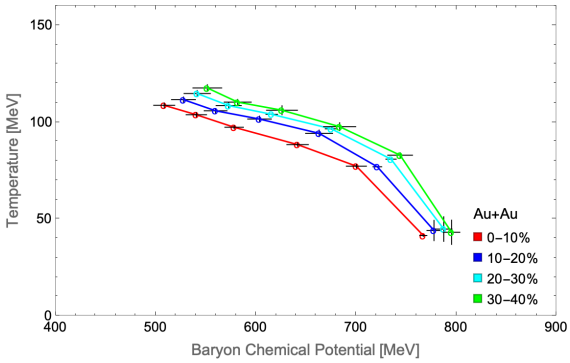

Fig. 1: *Chemical freeze out Temperatures and Baryon Chemical Potentials for Au+Au collisions at different centralities.*

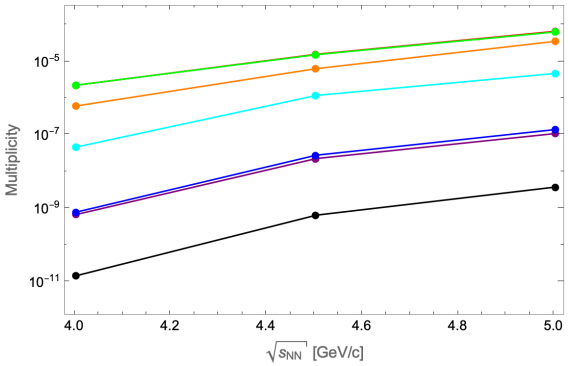

Fig. 2: *Particle multiplicities in central Au-Au collisions.*

simulations. We will employ the latest version v4.0 of the UrQMD model [3, 4] which has been shown to give a good description of many hadron multiplicities and has also been extended to predict charm production in the SIS100 energy range [5].

From UrQMD the following hadron multiplicities have been simulated for Au+Au collisions at SIS100 energies in four different centrality classes: 0–10%, 10–20%, 20–30%, and 30–40%:

- π^+, π^-, K^+, K^-, p, $\bar{p}$, Λ, $\bar{\Lambda}$, Ξ^-, Ω, and K^0_S and charmed hadrons $J/\psi, \Lambda_c$, obtained from UrQMD simulations of Au+Au collisions at different center-of-mass energies: 2.4, 3.0, 3.5, 4.0, 4.5, and 5.0 GeV.

The obtained multiplicities were then fitted within the (charm canonical) Statistical Hadronization Model (SHM) using the Thermal-FIST program [6]. The fit yields the chemical freeze-out temperature (T) and the baryon chemical potential (μ_B) for each centrality class and energy point. The fit parameters are shown in figure 1.

The plot clearly demonstrates that as the Baryon Chemical Potential (μ_B) increases (corresponding to lower collision energies), the Temperature (T) of the system at freeze-out decreases significantly.

When analyzing the different centrality classes (0–10%, 10–20%, 20–30%, and 30–40%), we observe that the more peripheral collisions (higher centrality percentages) tend to have slightly higher temperatures for a given (μ_B). However, the overall trend remains consistent across all centrality classes.

In addition to Au+Au collisions below the charm production threshold we also performed minimum bias simulations of proton+Au collisions at $\sqrt{s_{NN}} = 5.62$ GeV which would provide a much cleaner system for charmed hadron detection.

Finally, using available data from the ALICE collaboration on hadron and charm production in Pb+Pb collisions at $\sqrt{s_{NN}} = 5.02$ TeV, [7] [8] [9] [10] (including J/ψ, Λ_c, D mesons, D_s, and excited charmonium states) we are also able to predict exotica production using the chemical freeze-out temperature of $T_c = 156$ MeV.

3.1 Extension of the hadron spectrum of FIST

Several exotic charmed hadrons and nuclei are not yet included in the Thermal-FIST program and had to be added to the particle list by specifying their mass, charge, baryon number, strangeness, charm, and $|C|$. Table 1 lists the properties of the charmed hadrons and nuclei which have been added of for which predictions are then made within thermal-FIST. Note that nuclei are represented with curly brackets.

4 Results and discussion

In the following we will present the predictions for charmed exotics and nuclei production based on the input discussed above and thermal-FIST.

Firstly, figure 2 shows the multiplicity of several charmed exotica for most central (0-10%) Au+Au collisions as function of the beam energy (in the SIS100 beam energy range). Only selected Au+Au energies (4.0, 4.5, and 5.0 GeV) were chosen as the multiplicity at even lower energies drops to low.

Figure 3 then shows the multiplicity of

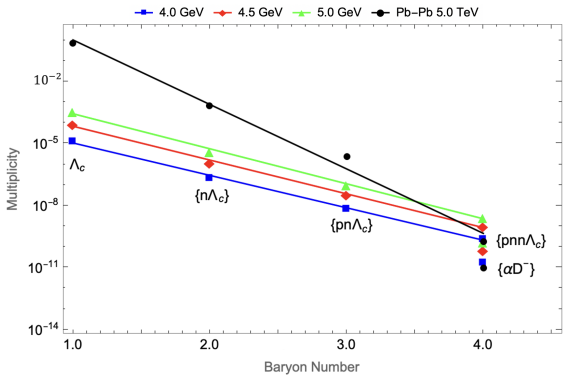

Fig. 3: *Particle multiplicities as a function of Baryon Number for Au+Au and Pb+Pb collisions.*

Particle	Au+Au	p+Au	Pb+Pb
$\{pn\Lambda_c\}$	2.153×10^{-7}	7.171×10^{-8}	4.910×10^{-6}
$\{n\Lambda_c\}$	1.256×10^{-5}	1.119×10^{-6}	0.002
$\{pnn\Lambda_c\}$	2.761×10^{-9}	3.510×10^{-9}	1.932×10^{-10}
$\{\alpha D^-\}$	3.597×10^{-10}	1.809×10^{-9}	1.867×10^{-11}
X(3872)	3.805×10^{-9}	4.509×10^{-8}	0.001
D_s^+	3.566×10^{-5}	5.489×10^{-7}	2.905
$\eta_c(1S)$	4.755×10^{-6}	9.242×10^{-6}	0.132
$\chi_{c0}(1P)$	1.092×10^{-7}	5.118×10^{-7}	0.010
$\chi_{c1}(1P)$	1.403×10^{-7}	7.931×10^{-7}	0.016
Σ_c^{++}	6.655×10^{-5}	2.167×10^{-6}	0.159
Σ_c^+	6.395×10^{-5}	2.065×10^{-6}	0.134

Tab. 2: *Predicted particle multiplicities in central Au+Au ($\sqrt{s_{NN}} = 5.0$ GeV), p+Au ($\sqrt{s_{NN}} = 5.62$ GeV), and central Pb+Pb collisions ($\sqrt{s_{NN}} = 5.02$ TeV).*

charmed nuclei as function of the baryon number for the three beam energies as blue, red and green symbols. The mass dependence shows a clear exponential suppression of the multiplicity with increasing baryon number of the produced states which is well known for light clusters.

In Pb+Pb collisions at 5.02 TeV (ALICE data), the multiplicities of charmed hadrons are higher by several orders of magnitude. This is expected since at FAIR/SIS100 energies the probability of producing sub-threshold charm should be strongly suppressed, while at LHC energies the production is much more favorable. The expected yields of exotic hadrons and charmed nuclei at the LHC is shown in table 2. In addition, the dependence of the charmed nuclei yields at the LHC is also shown in in figure 3. An interesting result here is that, for B=4 nuclei, the multiplicity at the LHC and SIS100 will become similar due to the abundance of baryons at the lower beam energies.

Finally, table 2 also lists the multiplicities expected in p+Au collisions at the SIS100, bit above the elementary charm production threshold. As can be seen the production probability is increased compared to the sub-threshold energies.

Particle	Mass[GeV]	Q	B	S	C	$\lvert C\rvert$
$\{pn\Lambda_c\}$	4.163	2	3	0	1	1
$\{n\Lambda_c\}$	3.225	1	2	0	1	1
$\{pnn\Lambda_c\}$	5.102	2	4	0	1	1
$\{\alpha D^-\}$	5.596	1	4	0	-1	1
X(3872)	3.872	0	0	0	0	2
D_s^+	1.968	1	0	1	1	1
$\eta_c(1S)$	2.984	0	0	0	0	2
$\chi_{c0}(1P)$	3.414	0	0	0	0	2
$\chi_{c1}(1P)$	3.510	0	0	0	0	2
Σ_c^{++}	2.454	2	1	0	1	1
Σ_c^+	2.453	1	1	0	1	1

Tab. 1: *List of charmed hadrons and nuclei that have been introduced to thermal-FIST with their masses and quantum numbers.*

5 Conclusion

In this work, we used the thermal model to predict the production of charmed hadrons nuclei in heavy-ion and proton-ion collisions at the SIS100 and LHC. While the production rate of charm is, as expected, much higher at the LHC, charmed exotica production may still be feasible with CBM@FAIR. The multiplicity of exotic states exhibits an exponential suppression with increasing baryon number which is stronger for the highest beam energies. These predictions provide a baseline reference for future studies of exotic and charm production in upcoming FAIR experiments, and they help to bridge the comparison between low and high-energy heavy-ion collisions.

Acknowledgments

I would like to express my sincere gratitude to my supervisor, Dr. Jan Steinheimer, for his invaluable guidance and continuous support throughout this work. I also thank B. Doenigus and V. Vovchenko for fruitfull discussions and help with the thermal-FIST program.

References

[1] F. Becattini, [arXiv:0901.3643 [hep-ph]].

[2] A. Andronic, P. Braun-Munzinger, M. K. Köhler, K. Redlich and J. Stachel, Phys. Lett. B **797**, 134836 (2019) doi:10.1016/j.physletb.2019.134836.

[3] S. A. Bass, *et al.* Prog. Part. Nucl. Phys. **41**, 255-369 (1998) doi:10.1016/S0146-6410(98)00058-1.

[4] M. Bleicher, *et al.* J. Phys. G **25**, 1859-1896 (1999) doi:10.1088/0954-3899/25/9/308.

[5] J. Steinheimer, A. Botvina and M. Bleicher, Phys. Rev. C **95**, no.1, 014911 (2017) doi:10.1103/PhysRevC.95.014911.

[6] V. Vovchenko and H. Stoecker, Comput. Phys. Commun. **244**, 295-310 (2019) doi:10.1016/j.cpc.2019.06.024

[7] ALICE Collaboration, S. Acharya et al., JHEP **01**, 174 (2022).

[8] ALICE Collaboration, S. Acharya et al., *Phys. Lett.* B **827**, 136986 (2022).

[9] ALICE Collaboration, S. Acharya et al., *Phys. Lett.* B **839**, 137796 (2023).

[10] ALICE Collaboration, S. Acharya et al., *Phys. Lett.* B **849**, 138451 (2024).